

A new role for Nogo as a regulator of vascular remodeling

Lisette Acevedo^{1,4}, Jun Yu^{1,4}, Hediye Erdjument-Bromage², Robert Qing Miao¹, Ji-Eun Kim³, David Fulton¹, Paul Tempst², Stephen M Strittmatter³ & William C Sessa¹

Although Nogo-A has been identified in the central nervous system as an inhibitor of axonal regeneration, the peripheral roles of Nogo isoforms remain virtually unknown. Here, using a proteomic analysis to identify proteins enriched in caveolae and/or lipid rafts (CEM/LR), we show that Nogo-B is highly expressed in cultured endothelial and smooth muscle cells, as well as in intact blood vessels. The N terminus of Nogo-B promotes the migration of endothelial cells but inhibits the migration of vascular smooth muscle (VSM) cells, processes necessary for vascular remodeling. Vascular injury in Nogo-A/B-deficient mice promotes exaggerated neointimal proliferation, and adenoviral-mediated gene transfer of Nogo-B rescues the abnormal vascular expansion in those knockout mice. Our discovery that Nogo-B is a regulator of vascular homeostasis and remodeling broadens the functional scope of this family of proteins.

The Nogo isoforms A, B and C are members of the reticulon family of proteins. Nogo-A and Nogo-C are highly expressed in the central nervous system, with Nogo-C being additionally found in skeletal muscle, whereas Nogo-B is found in most tissues^{1,2}. Nogo-A, produced in oligodendrocytes, was identified as an inhibitor of axonal growth and repair. After injury in mice, axon regeneration can be promoted by neutralizing Nogo-A function with antibodies that target its N terminus^{3,4}, or by antagonizing the binding of the Nogo loop domain (Nogo-66) to its cognate receptor, NgR⁵. More recently, some groups have found that the genetic loss of Nogo-A/B hastens axon repair after injury^{6,7}, although another group has not⁸. Given the considerable importance of understanding Nogo-mediated processes in the nervous system, little attention has been paid to the function or significance of Nogo isoforms in non-neural tissues.

Here we isolate highly purified, caveolin-1-containing, cholesterol-rich, buoyant membrane microdomains (CEM/LR) from endothelial cells. Proteomic analysis using previously established mass spectrometric procedures⁹ identifies Nogo-B in these membrane subfractions. We report that Nogo-B is highly expressed in endothelial and smooth muscle cells of the vessel wall, and show that Nogo-B is a regulator of cell migration *in vitro* and vascular remodeling *in vivo*.

RESULTS

Identification of Nogo-B in endothelial and VSM cells

CEM/LR were isolated from the human endothelial cell line EA.hy.926 and run on an SDS-PAGE gradient gel, and the 30 most prominent bands were excised for MALDI-reTOF mass spectrometry. One of the proteins identified by mass spectrometric fingerprint of multiple peptides was Nogo-B (data not shown). RT-PCR analysis of total RNA isolated from EA.hy.926 cells and from primary cul-

tures of human umbilical vein endothelial cells (HUVECs) detected the expression of Nogo-A, total Nogo-B and Nogo-B2 mRNA in endothelial cells (Fig. 1a). Plasmids expressing the cDNA encoding human Nogo-A and Nogo-B were used as positive controls. In contrast, western blotting with α -Nogo(1–18), an antibody recognizing amino acids 1–18 of the N terminus of both Nogo-A and Nogo-B, detected only the Nogo-B protein in EA.hy.926 cells and HUVECs (Fig. 1b). In human aortic VSM cells, α -Nogo(1–18) detected two bands migrating at the molecular weight of Nogo-B, suggesting that the variant Nogo-B2 was expressed in those cells. In control experiments, only Nogo-A protein or Nogo-B protein was detected in cells transfected with the cDNA encoding Nogo-A or Nogo-B, respectively. Similar observations of Nogo-A mRNA, but not protein, expression in various tissues have been reported¹⁰.

After sucrose gradient fractionation of endothelial cell membranes, the CEM/LR (fractions 2–4; Fig. 1c) was enriched in caveolin-1, but lacking in markers for bulk plasma membrane, angiotensin-converting enzyme (ACE) and Golgi/post-Golgi membranes (β -coatamer protein, B-cop). Western blot analysis confirmed that Nogo-B was enriched in the CEM/LR (Fig. 1c). To confirm that the Nogo-B in CEM/LR is indeed located in the plasma membrane, we first isolated a pellet containing plasma membrane, then isolated CEM/LR from this material by sucrose gradient fractionation. Nogo-B, caveolin-1, ACE and calnexin (an endoplasmic reticulum marker protein) were all found in the starting material (postnuclear supernatant; Fig. 1d). Nogo-B, caveolin-1 and ACE were present in the isolated plasma membrane pellet, and were de-enriched in the postmembrane supernatant. Residual Nogo-B cosedimented with calnexin in the postmembrane supernatant, consistent with the previously described localization of Nogo-A protein in the endoplasmic reticulum¹. Additional isola-

¹Department of Pharmacology and Program in Vascular Cell Signaling and Therapeutics, Boyer Center for Molecular Medicine, Yale University School of Medicine, New Haven, Connecticut 06536, USA. ²Molecular Biology Program, Memorial Sloan-Kettering Cancer Center, New York, New York 10021, USA. ³Neurology and Neurobiology, Yale University School of Medicine, New Haven, Connecticut 06536, USA. ⁴These authors contributed equally to this work. Correspondence should be addressed to W.C.S. (william.sessa@yale.edu).

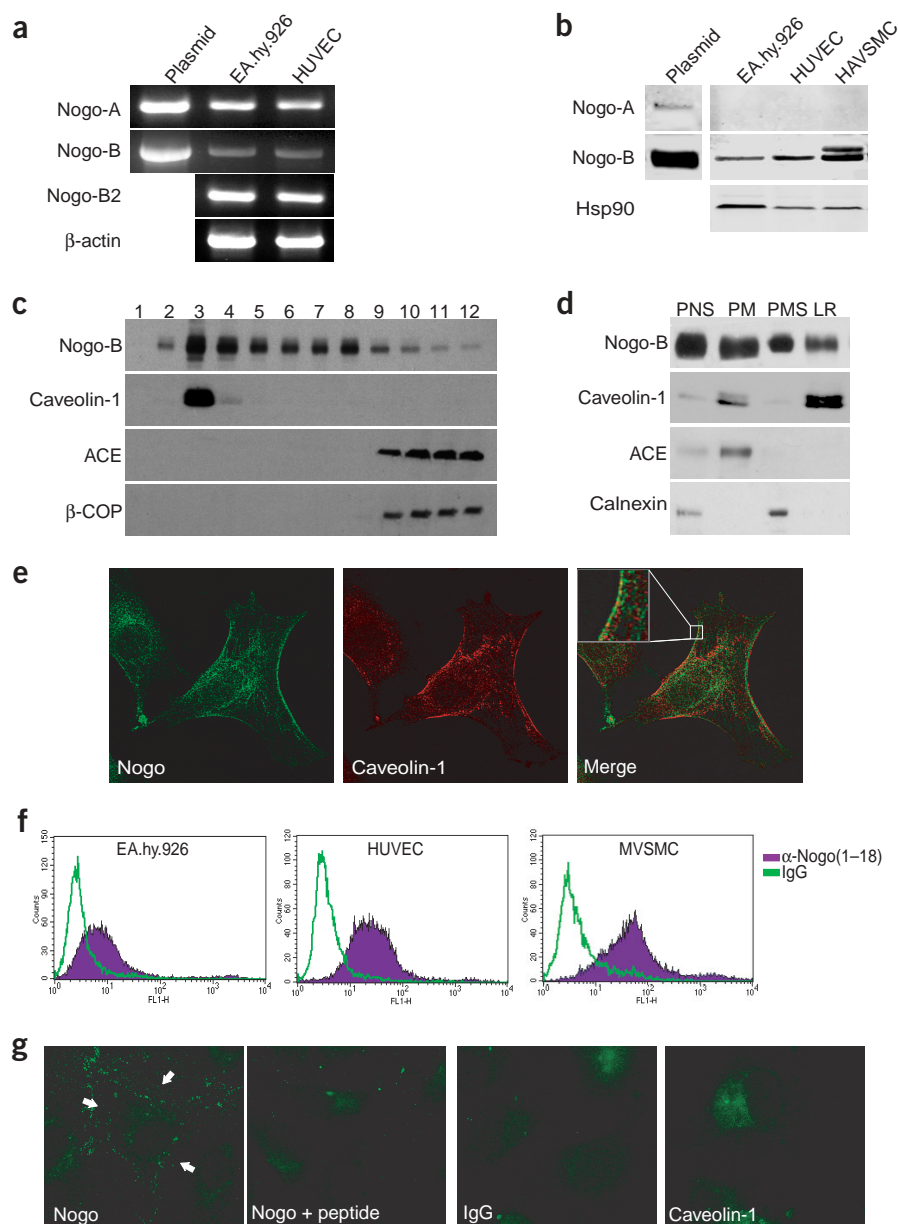


Figure 1 Identification of Nogo-B in vascular cells. **(a)** mRNA for Nogo isoforms in endothelial cells was detected by RT-PCR using isoform specific primers. Nogo-A or Nogo-B plasmids were used as controls. **(b)** Expression of Nogo proteins in transfected COS-7 cells expressing Nogo-A or Nogo-B, and in EA.hy.926 cells, HUVECs and human aortic VSM cells (HAVSMC). Protein expression was monitored using α -Nogo(1–18); Nogo-A and Nogo-B were distinguished based on molecular weight. Heat shock protein 90 (Hsp90) was used as a loading control. **(c)** Enrichment of Nogo-B in CEM/LR in EA.hy.926 cells. Equal volumes of sample were loaded from each fraction, and proteins were blotted with α -Nogo(1–18) and antibodies to caveolin-1, ACE and β -COP to determine the location of these protein markers. **(d)** Localization of Nogo-B in plasmalemmal CEM/LR of EA.hy.926 cells. Equal amounts of protein (5 μ g) in postnuclear supernatant (PNS), plasma membrane pellet (PM) and postmembrane supernatant (PMS) were loaded; the volume of the LR fraction loaded was equal to that of the PM fraction (50 μ l of each). **(e)** Colocalization of Nogo-B and caveolin-1 in EA.hy.926 cells, as detected by immunofluorescence microscopy (inset, $\times 63$ magnification). **(f)** FACS analysis of surface labeling of Nogo-B in EA.hy.926 cells, HUVECs and mouse VSM cells (MVSMC). **(g)** Surface staining for Nogo-B in EA.hy.926 cells, using immunofluorescent microscopy ($\times 63$ magnification).

tion of buoyant-density membranes from the plasma membrane fraction, identified by the presence of caveolin-1 and absence of ACE, confirmed the presence of Nogo-B in plasmalemmal CEM/LR. This localization was further supported by immunofluorescence microscopy, which showed colocalization of Nogo-B and caveolin-1 in permeabilized endothelial cells (Fig. 1e), and a predominantly reticular pattern of Nogo-B expression with some plasma membrane staining.

There are two possible topographies of Nogo-A in the plasma membrane—either its N terminus or its loop domain can be oriented extracellularly^{11,12}. We determined the orientation of Nogo-B in the plasma membrane by fluorescence-activated cell sorting (FACS) analysis of nonpermeabilized EA.hy.926, HUVEC and VSM cells, using α -Nogo(1–18) or nonimmune primary IgG as a control. The increase in fluorescence of cells stained with α -Nogo(1–18) indicated the presence of Nogo-B on the cell surface, with its N terminus oriented extracellularly in all three cell types (Fig. 1f). In

additional experiments using FACS analysis in permeabilized cells, the cell surface staining reflected $\sim 2\%$ of the total Nogo-B pool (data not shown). Immunofluorescence microscopy of non-permeabilized endothelial cells showed that α -Nogo(1–18) labeled the cell surface in a punctate manner, consistent with the localization of protein in patches on the cell surface (Fig. 1g). The cell surface labeling of Nogo-B was eliminated by addition of the Nogo(1–18) peptide used as the immunogen and no staining was seen

Analysis of Nogo-B function

Because of the extracellular orientation of the N terminus of Nogo-B observed in endothelial cells, we studied the effects of this domain on vascular cells using a glutathione S-transferase fusion protein encompassing the N-terminal residues 1–200 (GST-Am-Nogo-B; Fig. 2a). Previous studies have shown that a fusion protein containing the N terminus of Nogo-A, specifically amino acids 59–172 (residues in common with Nogo-B) and 544–725 (residues unique to Nogo-A), inhibits the spreading of various cell types, whereas the Nogo-66 loop domain inhibits the spreading specifically of neurons^{12,13}. To characterize the activity of Nogo-B on vascular cell

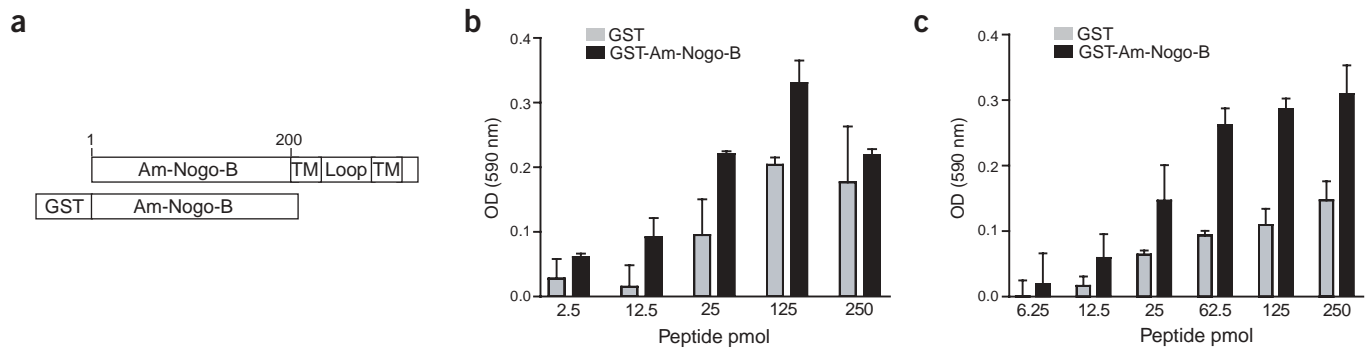


Figure 2 The N terminus of Nogo-B promotes vascular cell adhesion. **(a)** Diagram of primary amino acid domains of Nogo-B used to generate GST-Am-Nogo-B. TM, transmembrane domains; loop, Nogo-66. **(b,c)** GST-Am-Nogo-B promoted adhesion of EA.hy.926 endothelial cells **(b)** and rat arterial smooth muscle cells **(c)** in a dose-dependent manner. Data represent mean \pm s.e.m. from experiment done in quadruplicate. Experiment was repeated three additional times with similar results.

function, we examined whether GST-Am-Nogo-B influences endothelial and VSM cell adhesion. Coating plates with GST-Am-Nogo-B, but not GST alone, caused a dose-dependent increase in the adhesion of both EA.hy.926 and rat aortic smooth muscle cells (Fig. 2b,c). Identical results were observed using HUVECs (data not shown). These data show that Am-Nogo-B(1–200) is a functional domain for Nogo-mediated signaling in endothelial and VSM cells.

Am-Nogo-B regulates cell migration

We next examined whether the soluble N terminus of Nogo-B could serve as a chemoattractant for endothelial cells. We cultured HUVECs on Transwell inserts, and added GST, GST-Am-Nogo-B or vascular endothelial growth factor (VEGF; used as a positive control) to the bottom wells of the chambers to establish a gradient. GST-Am-Nogo-B, but not GST, dose-dependently increased endothelial cell migration (Fig. 3a). Addition of GST-Am-Nogo-B or VEGF to both the upper and lower chambers, thereby eliminating the chemoattractant gradient, abolished directional migration.

Previous work on Nogo-A has shown that a soluble form of Nogo-66 generated by a secreted alkaline phosphatase (AP) fusion protein is biologically active¹³. We used AP-Am-Nogo-B to examine the chemotactic function of Am-Nogo-B(1–200) in endothelial and VSM cells. Purified AP-Am-Nogo-B (10 nM), but not alkaline phosphatase alone, promoted the migration of endothelial cells (Fig. 3b) in a manner similar to GST-Am-Nogo-B (Fig. 3a). In contrast, AP-Am-Nogo-B (50

nM) did not promote the migration of VSM cells (Fig. 3c), but dose-dependently blocked the VSM cell migration induced by platelet-derived growth factor-BB (PDGF-BB; 15 ng/ml). AP-Am Nogo-B also blocked VSM cell migration in response to varying concentrations of PDGF (5–15 ng/ml; **Supplementary Fig. 1** online). Alkaline phosphatase alone (50 nM) did not influence migration *per se*, or the response to PDGF-BB. These data indicate that Nogo-B can exert differential actions on the migration of endothelial and VSM cells.

To examine whether the N terminus of Nogo-B could potentially exert its biological effects through the cloned Nogo-66 receptor NgR¹³, we examined the cell surface binding of AP-Am-Nogo-B and AP-Nogo-66 in COS-7 cells transiently expressing the cDNA encoding NgR. Transfection of NgR resulted in the specific cell surface

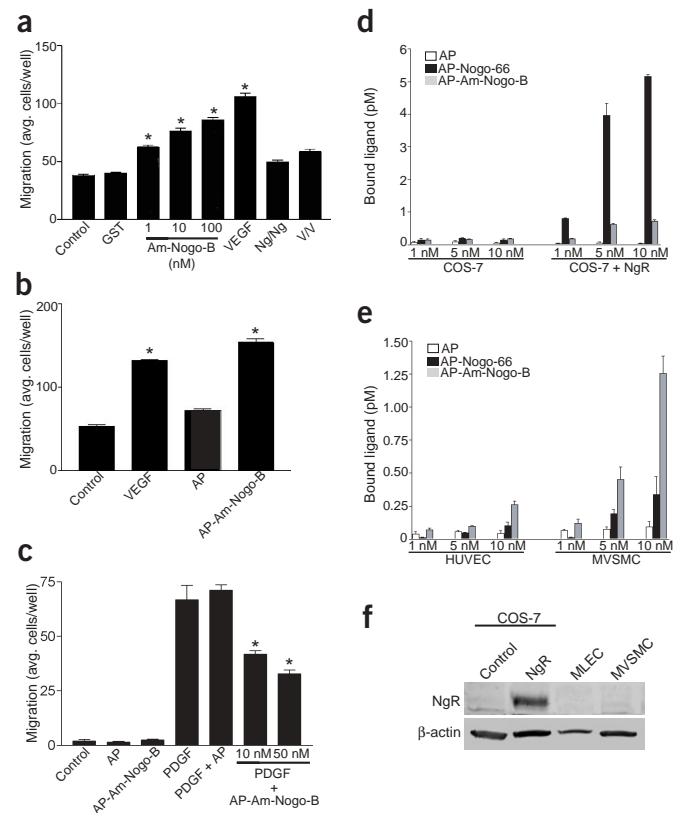


Figure 3 Am-Nogo-B is a chemoattractant for HUVECs. **(a)** HUVEC migration was examined in modified Boyden chambers using recombinant GST, GST-Am-Nogo-B and VEGF (1.1 nM). Ng/Ng and V/V indicate experiments in which Am-Nogo-B (10 nM) or VEGF (1.1 nM), respectively, were added to both chambers. **(b)** Cell migration was examined as above using alkaline phosphatase (AP), AP-Am-Nogo-B and VEGF (as a positive control). **(c)** AP-Am-Nogo-B is an inhibitor of VSM cell migration. Cells were treated with AP or AP-Am-Nogo-B (each 50 nM), alone or with the chemoattractant PDGF-BB (15 ng/ml). Each value in **a–c** represents mean \pm s.e.m. (in triplicate). Experiments were repeated an additional three times, with similar results. *, $P < 0.05$ compared with GST alone **(a)**, control and AP **(b)**, or PDGF or PDGF + AP **(c)**. **(d,e)** Surface binding of AP, AP-Nogo-66 and AP-Am-Nogo-B to COS-7 cells transfected with NgR **(d)**, or native HUVECs and mouse VSM cells (MVSMC; **e**). Data in **d** and **e** represent mean \pm s.e.m. from an experiment done in triplicate. **(f)** Lack of NgR expression in vascular cells. Western blot analysis of NgR expression in 30- μ g protein extracts from mouse lung endothelial cells (MLEC) and MVSMC, and from COS-7 cells transfected with cDNA encoding NgR. β -actin is used as loading control.

binding of AP-Nogo-66, with little binding of AP-Am-Nogo-B and negligible binding of alkaline phosphatase alone (Fig. 3d). In contrast, AP-Am-Nogo-B, but not AP-Nogo-66 or alkaline phosphatase alone, bound to the cell surface of endothelial cells and, to a greater extent, to the surface of VSM cells (Fig. 3e). Using an antibody to mouse NgR, we examined NgR expression in mouse lung endothelial cells (MLEC) and mouse VSM cells. NgR was not detectable in mouse lung endothelial or VSM cells, but was readily detectable in COS-7 cells transfected with mouse NgR (Fig. 3f). Thus, AP-Am-Nogo-B and AP-Nogo-66 bind differently to NgR expressed in COS-7 cells, and bind differently to vascular cells. Together with the relative paucity of NgR expression in primary cultures of endothelial and VSM cells, these findings suggest that Am-Nogo-B may bind to a different cell surface receptor in vascular cells.

Nogo-A/B isoforms are highly expressed in blood vessels *in vivo*

To examine the *in vivo* role of Nogo in the vasculature, we first assessed the expression of Nogo isoforms in blood vessels obtained from mice. Using specific primers for total Nogo-B, Nogo-B2, Nogo-A and Nogo-C, we found that mRNA encoding all isoforms was expressed in mouse brain, femoral and carotid arteries and in the thoracic and abdominal aorta (Fig. 4a). Western blotting of cell extracts from these tissues detected the expression of Nogo-B protein in isolated blood vessels, whereas Nogo-A was enriched only in brain extracts (Fig. 4b). To examine the tissue distribution of Nogo-A/B *in vivo*, we used mice with a targeted gene trap of the locus encoding Nogo-A/B⁶. The gene trap is located at the 5' end of the largest Nogo-A-selective exon, and disrupts the expression of Nogo-

A and Nogo-B, but not Nogo-C. The Nogo-A/B-deficient mice were viable and fertile, and exhibited normal behavior as described^{6–8}. The β -galactosidase gene inserted into the Nogo-A/B-encoding locus was used to track the endogenous expression of Nogo-A/B. Nogo-A, but not Nogo-B, was highly expressed in brains of wild-type mice, whereas Nogo-B, but not Nogo-A, was highly expressed in the aorta (Fig. 4c). Disruption of the gene encoding Nogo-A/B resulted in the loss of immunoreactive Nogo-B from the aorta. β -galactosidase activity, an index of endogenous Nogo-A/B expression, was found in endothelial and VSM cells of the femoral artery and in the endothelium of the paired femoral vein (Fig. 4d), and in both layers of the aorta (Fig. 4e). Whole-mount staining showed that Nogo-A/B was expressed in large blood vessels emanating from the heart, and in the atria and main coronary vessels (Fig. 4f). Cross-sections through the atria showed transgene expression in atrial myocytes and coronary vessels and, more sparsely, in ventricular myocytes peripheral to the vessel (Fig. 4g). Additional staining was seen in most vascular tissues, including vessels in the brain (Fig. 4g), lung epithelium and VSM, and in epithelial cells of the lung, intestine and gall bladder (data not shown).

Nogo regulates vascular remodeling

Because Nogo-A/B-deficient mice are viable, these Nogo isoforms are not essential for vascular development; however, the expression of Nogo-B in the vessel wall, as well as its effects on endothelial and VSM cell function, suggests that it may influence several aspects of post-natal vascular homeostasis, including the response to injury and luminal remodeling. To examine the endogenous expression of Nogo-B and its regulation during injury-induced remodeling, we injured the femoral arteries of C57BL/6 mice and examined the temporal pattern of Nogo expression by immunofluorescence microscopy. Immunostaining of uninjured vessels with α -Nogo(1–18) detected Nogo expression in

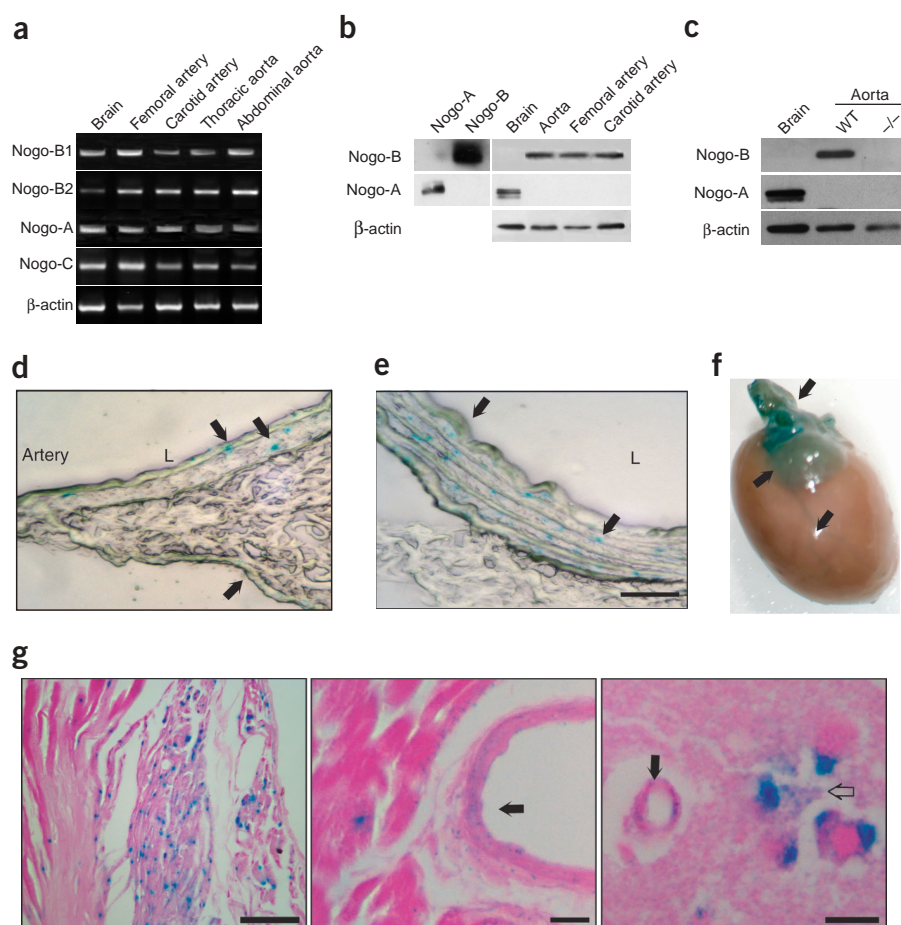


Figure 4 Nogo-B is present in intact blood vessels. (a) mRNA for various Nogo isoforms was detected in isolated mouse blood vessels by RT-PCR, using isoform-selective primers. (b) Nogo-B, but not Nogo-A, protein is expressed in mouse blood vessels. Lysates of mouse brain or COS-7 cells transfected with cDNA encoding Nogo-A or Nogo-B were used as antibody controls; β -actin was used as a loading control. (c) Nogo-A/B proteins are absent from brain and aortic extracts prepared from Nogo-A/B-deficient ($-/-$) mice. WT, wild type. Nogo-B was detected using α -Nogo(1–18); Nogo-A was detected using antibody to Nogo-A. (d,e) X-gal staining of femoral artery/vein pair (d) and aorta (e) isolated from Nogo-A/B-deficient mouse. L indicates vessel lumen; arrows indicate areas of gene expression in endothelium (d) and smooth muscle (e). Scale bar, 50 μ m. (f) Whole-mount staining of mouse heart. Arrows indicate areas of gene expression in large vessels, main coronary artery, left anterior descending vessel and atria. (g) Cross-sections showing Nogo-A/B expression in atrial myocytes (left), coronary vessels (middle; black arrow) and cerebral cortex (right; open arrow indicates neurons). Scale bars, 50 μ m (left) or 10 μ m (middle and right).

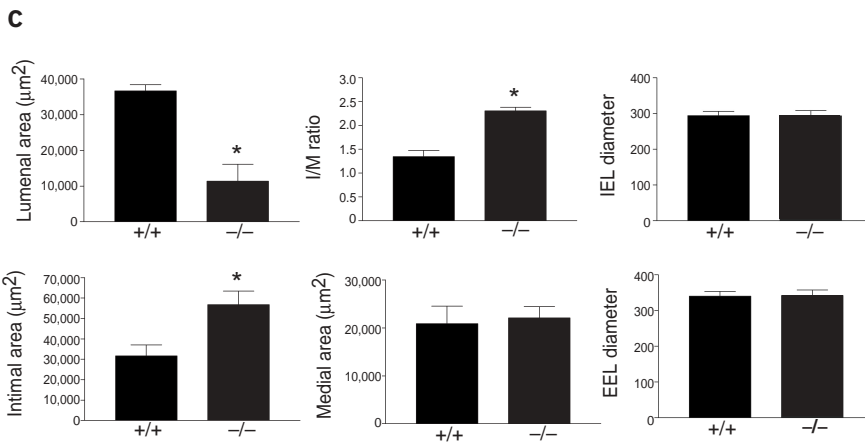
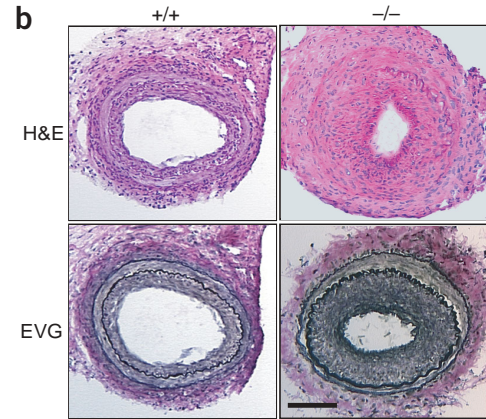
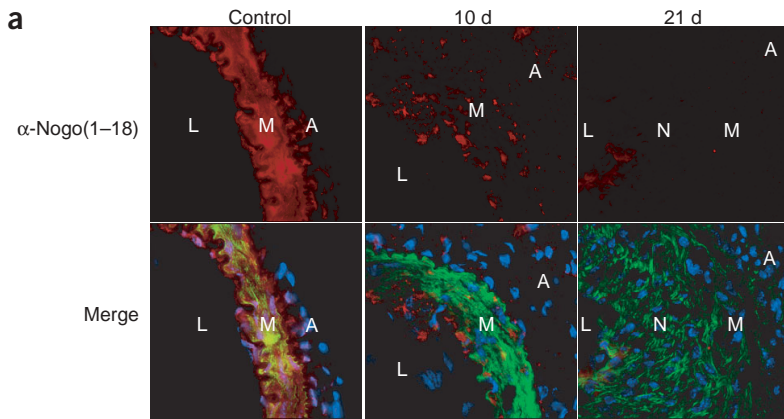


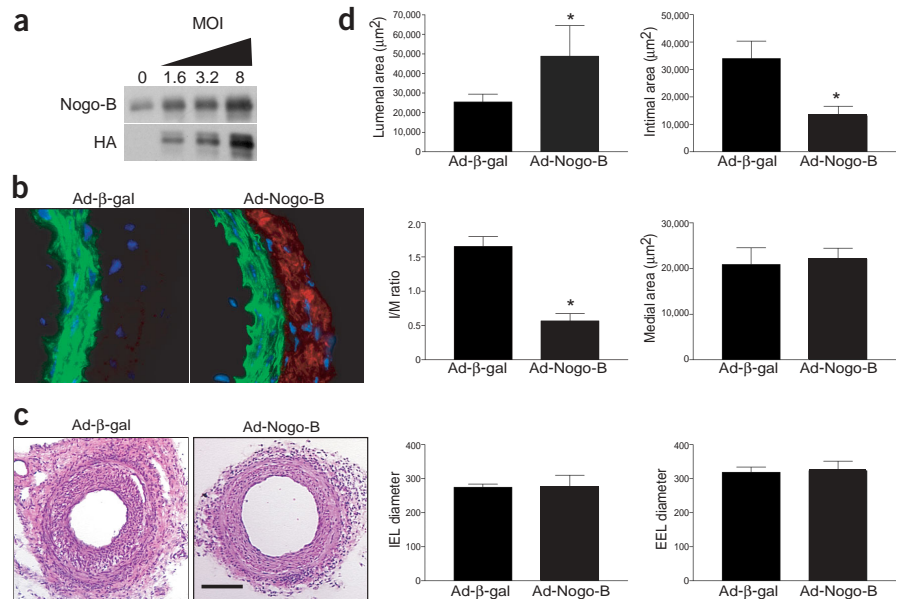
Figure 5 Evidence supporting a role for Nogo in vascular remodeling. (a) Vascular injury reduces immunoreactive Nogo in vessel walls. Shown are femoral artery sections, uninjured (control) or 10 and 21 d after injury, stained with α -Nogo(1–18) (red) alone or together with FITC-conjugated phalloidin (green) and DAPI (blue). L, lumen; M, media; A, adventitia; N, neointima. Magnification, $\times 63$. (b) Loss of Nogo promotes pathological inward remodeling. H&E and elastic von Giessen (EVG; delineates elastic laminae) staining of femoral arteries obtained from wild-type (+/+) and Nogo-A/B-deficient (-/-) mice, 3 weeks after injury. Scale bar, 100 μ m. (c) Quantitative morphometry of vessel remodeling in Nogo-A/B-deficient mice and wild-type littermates, 3 weeks after injury. Data are expressed as mean \pm s.e.m. of ten sections from each of four vessels. *, $P < 0.05$. Similar results were obtained in a separate cohort of mice.

endothelial cells lining the lumen and VSM cells of the media (Fig. 5a). Ten days after injury, there was a marked loss of Nogo immunoreactivity in the media of the injured vessel during the early stages of medial expansion; immunoreactive Nogo was virtually absent after 21 d of neointimal expansion (Fig. 5a). These data sug-

gest that Nogo disappeared from the vessel wall as a consequence of vessel injury, and that its loss correlated with neointima formation.

To examine directly whether the genetic loss of Nogo-B influences the magnitude of injury-induced vascular remodeling, we injured the femoral arteries of Nogo-A/B-deficient mice and their age- and

Figure 6 Reconstitution with Ad-Nogo-B prevents injury-induced neointimal expansion in Nogo-A/B-deficient mice. (a) Characterization of adenovirus expressing HA-Nogo-B. EA.hy.926 cells were infected with increasing multiplicity of infection (MOI) of Ad-Nogo-B. Cell extracts were blotted with α -Nogo(1–18) and antibody to hemagglutinin. (b) Immunofluorescent staining with antibody to hemagglutinin shows localization of virally expressed protein (red) within transduced vessels. Vessels were counterstained with FITC-conjugated phalloidin (green) and DAPI (blue) to delineate cells. Magnification, $\times 63$. (c) H&E staining of arteries in which VSM cells were transduced with Ad- β -gal and Ad-Nogo-B. Neointima is thickened in segments transduced with Ad- β -gal, compared with segments transduced with Ad-Nogo-B. Scale bar, 100 μ m. (d) Quantitative morphometry of vessel remodeling in Nogo-A/B-deficient mice transduced with viral vectors, 3 weeks after injury. Data are expressed as mean \pm s.e.m. of ten sections from each of four vessels. *, $P < 0.05$.



sex-matched wild-type littermates. Three weeks after injury, the mutant mice showed markedly enhanced neointima formation and, in some cases, complete occlusion of the femoral artery, compared with the littermate control mice (Fig. 5b). There was no overall change in the cellular composition of lesions from control mice or mice lacking Nogo-A/B (Supplementary Fig. 2 online). All Nogo-A/B-deficient mice exhibited a blackening of the toes after injury, consistent with flow-limiting stenosis in the injured femoral artery. Quantitative morphometry of the injured vessels revealed a marked reduction in luminal area and an increase in neointimal expansion (that is, increased intimal area and intimal/medial (I/M) ratio), with no changes in medial area or overall vessel size (IEL and EEL diameters), in injured vessels from knockout mice compared with those from littermate controls (Fig. 5c). These morphometric measurements are consistent with marked pathological inward remodeling.

To further investigate whether Nogo-B is crucial for limiting vascular injury, we generated an adenoviral construct (Ad-Nogo-B) expressing a hemagglutinin-tagged form of Nogo-B, Nogo-B-HA. Infection of endothelial cells with increasing titers of Ad-Nogo-B resulted in increased expression of the transgene (Fig. 6a). We then introduced Ad-Nogo-B or adenoviruses expressing β -galactosidase (Ad- β -gal) into pluronic acid gels, and applied them to the adventitial side of the vessel walls of Nogo-A/B-deficient mice immediately after wire injury. As in our previous paper using a green fluorescent protein-expressing adenovirus to quantify the magnitude of gene expression¹⁴, transduction of the femoral artery with Ad-Nogo-B resulted in expression of Nogo-B-HA after 1 week, primarily in the adventitia (Fig. 6b) but with lesser expression in the media of the injured vessel, thus confirming the delivery and expression of the transgene *in vivo*. Injured femoral arteries from Nogo-A/B-deficient mice transduced with Ad- β -gal showed substantial neointima formation (Fig. 6c), as quantified by a decrease in luminal area and an increase in intimal expansion (intimal area and I/M ratios 3 weeks after injury). In contrast, injured arteries transduced with Ad-Nogo-B showed a marked reduction in gross injury (Fig. 6c), neointimal area and I/M ratio (Fig. 6d). These data suggest that transduction of vessels with Ad-Nogo-B rescues the deficiency in Nogo-A/B proteins, thus supporting the concept that endogenous expression of Nogo-B is important for vascular maintenance and remodeling.

DISCUSSION

This study identifies Nogo-B as a regulator of vascular function, thereby providing evidence for a peripheral role of this Nogo isoform. Previous work has focused on the biology of Nogo-A, Nogo-A receptors and Nogo-A coreceptors as negative regulators of axonal regeneration in the central nervous system. Despite the ubiquitous presence of Nogo mRNA in a variety of cultured cells, no functional role had yet been ascribed to Nogo-B *in vitro* or *in vivo*. Our study shows that Nogo-B protein is highly enriched in blood vessels, and that the genetic loss of Nogo-A/B expression markedly augments the injury response in femoral arteries. Thus, the Nogo family of proteins has an unanticipated role in vascular control.

Our identification of Nogo-B in endothelial cells using a proteomic screen for proteins enriched in CEM/LR provides a salient example of the use of proteomics to promote inductive scientific discovery. Nogo-B was found on the cell surface, with its N terminus oriented extracellularly. This work is consistent with findings on Nogo-A, whose biological activity in neurons has been ascribed to only its extracellular portions (either the N terminus or Nogo-66), even though most of the protein is found in the endoplasmic reticulum^{1,5,12,15}. It is not known how the extracellular domains of

Nogo-A or Nogo-B become exposed and released upon injury, or how they engage in receptor-dependent signaling, but this is an active area of investigation. Surprisingly, our *in vitro* biological activity data differ from the known inhibitory roles of Nogo-A in multiple cell types. In contrast, the N terminus of Nogo-B, which shares identical residues with the N terminus of Nogo-A, promotes the *in vitro* adhesion of endothelial and VSM cells. The N terminus of Nogo-B can also act as a chemoattractant for endothelial cells, similar to VEGF. The Nogo-B N terminus also antagonizes PDGF-stimulated migration of smooth muscle, an effect that might occur by competitive antagonism of PDGF receptor binding, or by functional blockade of PDGF signaling downstream of the receptor. The Nogo isoforms may exert cell- and tissue-specific effects, considering the restricted patterns of Nogo-A/B expression, and Nogo-A and Nogo-B may signal through different receptor subtypes. These contentions are supported by our data documenting the expression of Nogo-B protein in all the vessels studied, the lack of NgR expression in endothelial and smooth muscle cells, and the apparently different binding sites for AP-Am-Nogo-B compared with AP-Nogo-66 on endothelial and VSM cells.

The biological significance of Nogo-B in blood vessels is underscored by its endogenous expression in arteries and veins of multiple organs, and by the marked neointimal expansion in injured vessels of Nogo-A/B-deficient mice. Mechanistically, *in vitro* data shows that the N terminus of Nogo-B promotes vascular cell adhesion, stimulates endothelial cell migration and blunts PDGF-induced smooth muscle migration. These attributes are consistent with the idea that endogenous Nogo may contribute to vascular maintenance or quiescence in postnatal mice. The actions of Nogo-B are likely to be permissive, as there was no gross abnormality in vessel dimensions of arteries from Nogo-A/B-deficient mice. In normal mice, there was a marked loss of Nogo-B from the medial layer and a delayed loss of Nogo-B from the endothelium after injury, suggesting that the loss of Nogo-B may contribute to early phases of neointima formation. The permissive actions of Nogo-B were overtly manifested in injured vessels from Nogo-A/B-deficient mice, in which the complete loss of Nogo promoted abnormal neointima formation to the point where the lesions became stenotic, as evidenced by the gangrenous toes seen only in the mutant mice. These effects were presumably caused by a slower or impaired re-endothelialization process, and/or the loss of a negative regulator of growth factor-driven VSM migration and organization. The finding that neointima formation was corrected by Ad-Nogo-B in injured vessels of Nogo-A/B-deficient mice strongly supports a causal role for Nogo-B in this response. Our interpretation is that Nogo-B promotes endothelial cell recovery and blocks PDGF signaling in adventitia or smooth muscle. At the present time, however, we cannot assess the relative importance of Nogo in endothelium compared with VSM, nor can we rule out the possibility that Nogo-B negatively regulates stem cell mobilization, cell growth, thrombosis or inflammation, additional attributes that would reduce neointima formation. The discovery of Nogo-B in vessels may enrich our understanding of the pathways that regulate tissue remodeling in disease states such as atherosclerosis, postangioplasty restenosis, diabetes and cancer.

METHODS

Expression vectors. The cDNA encoding Nogo-B was amplified by RT-PCR from EA.hy926 cells, and ligated into pcDNA3. GST-Am-Nogo-B was generated from the cDNA encoding Am-Nogo-B(1–200) and ligated into pGEX4T-1. AP-Am-Nogo-B was generated by ligating the cDNA encoding Am-Nogo-B(1–200) into

the vector pAP6. Ad-Nogo-B was generated as described¹⁶, by ligating hemagglutinin-tagged Nogo-B into pShuttleCMV. GST-Nogo-66, pcDNA3.1-MycHis-Nogo-A¹ and AP-Nogo-66 were generated as described¹³.

Western blot analysis. Nogo expression was detected using α -Nogo(1–18) (Santa Cruz Biotechnology) or antibody to Nogo-A¹⁷. We also used antibodies to β -actin (Sigma), heat-shock protein-90 (BD Biosciences PharMingen), ACE (QED Biosciences), β -COP (ABR) and hemagglutinin (Roche).

Isolation of CEM/LR and identification of Nogo-B. CEM/LR from EA.hy.926 cells was prepared as described¹⁸. To purify lipid microdomains, the buoyant membrane fraction from the first gradient was reloaded on a discontinuous sucrose gradient. CEM/LR was repelleted at 100,000 g, run on SDS-PAGE and stained with Coomassie blue. The most prominent proteins were digested with trypsin and fractionated, and the peptide mixtures were analyzed by MALDI-reTOF mass spectrometry (Reflex III, BRUKER Daltonics). Peptide mixtures were also analyzed using an electrospray ionization triple-quadrupole instrument (API300, ABI/MDS SCIEX) modified with an ultrafine ionization source⁹. Selected ion masses from the MALDI-reTOF MS or NanoES-MS/MS spectra were used to search a protein nonredundant database ('NRI', National Center for Biotechnology Information).

Plasmalemmal CEM/LR was isolated by homogenizing cells in Tris (pH 9.6) with 5 mM MgCl₂, and pelleted at 10,000 g to enrich plasma membrane markers compared with endoplasmic reticulum markers. The plasma membrane was resuspended in 500 mM sodium carbonate and processed as above to isolate CEM/LR.

Surface staining and FACS analysis. EA.hy.926 cells were incubated with 5 μ g of α -Nogo(1–18) or goat IgG (Santa Cruz Biotechnology) for 1 h at 4 °C, then fixed with 3% paraformaldehyde and further incubated with FITC-conjugated secondary antibody. For surface staining, antibody to caveolin-1, as well as addition of the peptide used to raise α -Nogo(1–18) (both from Santa Cruz), were used as controls. For FACS analysis, cells were detached using Versene (Bio-Whittaker), and an equal number of cells was treated as above. For permeabilization, 0.3% saponin was added with the antibodies.

Cell spreading, adhesion and migration assays. GST, GST-Am-Nogo-B or GST-Nogo-66 (125 pmol each) was added to cover slips coated with 0.02% poly-L-lysine, and dried overnight. Adherent EA.hy.926 cells (50,000 cells) were fixed and stained with Alexa 594-conjugated phalloidin (Molecular Probes), and 150–200 cells were counted per cover slip. Adhesion experiments were done essentially as described¹⁹, with minor modifications. Titered plates were coated as above, but with 25 pmol of protein. We plated 20,000 cells into each well and let them adhere for 1 h before fixation and quantitation. We used a modified Boyden chamber with Costar Transwell inserts (Corning) for migration experiments²⁰. The inserts were coated with a solution of 0.1% gelatin (Sigma). VEGF (50 ng/ml), GST (100 nM), recombinant GST-Am-Nogo-B (1–100 nM), alkaline phosphatase (10 nM) or AP-Am-Nogo-B (10 nM) were dissolved in Medium 199 containing 0.1% BSA, and added to the bottom chambers. HUVECs (2 \times 10⁵ cells) and VSM cells (1 \times 10⁵) were added to the upper chambers. After 5 h, cells on both sides of the membrane were fixed and stained with Diff-Quik staining kit (Baxter Healthcare). We counted the average number of cells from five randomly chosen high-power (\times 400) fields on the lower side of the membrane. For experiments with rat aortic smooth muscle cells migration, PDGF-BB (15 ng/ml) was dissolved in high-glucose DMEM and added to the bottom chambers. Alkaline phosphatase (50 nM) or AP-Am-Nogo-B (10 and 50 nM) was preincubated with 1 \times 10⁵ cells for 15 min before cells were added to the upper chambers and processed as above.

Alkaline phosphatase fusion protein binding. COS-7 cells were transiently transfected with cDNA encoding the Nogo-66 receptor NgR. Forty-eight hours after transfection, assays for AP-Am-Nogo-B binding were done as described²¹. Plates were incubated with 10 nM AP-Am-Nogo-B, AP-Nogo-66 or alkaline phosphatase conditioned medium in binding buffer at 4 °C for 2 h. Unbound proteins were removed, and bound proteins were solubilized in 1% Triton X-100. After vortexing vigorously, the nuclei were spun out and supernatants were heated for 10 min at 65 °C. Alkaline phosphatase activity was determined by measuring optical density at 410 nm, as described.

X-gal staining. Upon sacrifice, Nogo-A/B-deficient mice were perfusion-fixed with buffered 2% paraformaldehyde, and tissues were stained overnight at 37 °C.

Femoral artery injury and adenoviral transduction. All experiments were approved by the Institutional Animal Care and Use Committees of Yale University. Nogo-A/B-deficient mice were back-bred seven generations to a C57BL/6 background, and used to generate Nogo-A/B-deficient mice and wild-type littermates. Femoral arteries were injured as previously described^{14,22}. Immediately after injury, Ad- β -gal or Ad-Nogo-B (3 \times 10⁸ PFU) was delivered by painting the adventitial side of the femoral artery with 50 μ l of a mixture containing 15 μ l of adenovirus in 35 μ l of 30% Pluronic-127 gel (Sigma).

Note: Supplementary information is available on the Nature Medicine website.

ACKNOWLEDGMENTS

This work is supported by grants to W.C.S. from the National Heart, Lung and Blood Institute, and to P.T. from the National Cancer Institute.

COMPETING INTERESTS STATEMENT

The authors declare that they have no competing financial interests.

Received 31 October 2003; accepted 2 March 2004

Published online at <http://www.nature.com/naturemedicine/>

- GrandPre, T., Nakamura, F., Vartanian, T. & Strittmatter, S.M. Identification of the Nogo inhibitor of axon regeneration as a Reticulon protein. *Nature* **403**, 439–444 (2000).
- Chen, M.S. *et al.* Nogo-A is a myelin-associated neurite outgrowth inhibitor and an antigen for monoclonal antibody IN-1. *Nature* **403**, 434–439 (2000).
- Brosamle, C., Huber, A.B., Fiedler, M., Skerra, A. & Schwab, M.E. Regeneration of lesioned corticospinal tract fibers in the adult rat induced by a recombinant, humanized IN-1 antibody fragment. *J. Neurosci.* **20**, 8061–8068 (2000).
- Merkler, D. *et al.* Locomotor recovery in spinal cord-injured rats treated with an antibody neutralizing the myelin-associated neurite growth inhibitor Nogo-A. *J. Neurosci.* **21**, 3665–3673 (2001).
- GrandPre, T., Li, S. & Strittmatter, S.M. Nogo-66 receptor antagonist peptide promotes axonal regeneration. *Nature* **417**, 547–551 (2002).
- Kim, J.E., Li, S., GrandPre, T., Qiu, D. & Strittmatter, S.M. Axon regeneration in young adult mice lacking Nogo-A/B. *Neuron* **38**, 187–199 (2003).
- Simonen, M. *et al.* Systemic deletion of the myelin-associated outgrowth inhibitor Nogo-A improves regenerative and plastic responses after spinal cord injury. *Neuron* **38**, 201–211 (2003).
- Zheng, B. *et al.* Lack of enhanced spinal regeneration in Nogo-deficient mice. *Neuron* **38**, 213–224 (2003).
- Winkler, G.S. *et al.* Isolation and mass spectrometry of transcription factor complexes. *Methods* **26**, 260–269 (2002).
- Oertle, T., Huber, C., van der Putten, H. & Schwab, M.E. Genomic structure and functional characterisation of the promoters of human and mouse *nogo/rtn4*. *J. Mol. Biol.* **325**, 299–323 (2003).
- Filbin, M.T. Myelin-associated inhibitors of axonal regeneration in the adult mammalian CNS. *Nat. Rev. Neurosci.* **4**, 703–713 (2003).
- Oertle, T. *et al.* Nogo-A inhibits neurite outgrowth and cell spreading with three discrete regions. *J. Neurosci.* **23**, 5393–5406 (2003).
- Fournier, A.E., GrandPre, T. & Strittmatter, S.M. Identification of a receptor mediating Nogo-66 inhibition of axonal regeneration. *Nature* **409**, 341–346 (2001).
- Blanc-Brude, O.P. *et al.* Inhibitor of apoptosis protein survivin regulates vascular injury. *Nat. Med.* **8**, 987–994 (2002).
- Huber, A.B. & Schwab, M.E. Nogo-A, a potent inhibitor of neurite outgrowth and regeneration. *Biol. Chem.* **381**, 407–419 (2000).
- He, T.-C. *et al.* A simplified system for generating recombinant adenoviruses. *Proc. Natl. Acad. Sci. USA* **95**, 2509–2514 (1997).
- Wang, X. *et al.* Localization of Nogo-A and Nogo-66 receptor proteins at sites of axon-myelin and synaptic contact. *J. Neurosci.* **22**, 5505–5515 (2002).
- Song, K.S. *et al.* Co-purification and direct interaction of Ras with caveolin, an integral membrane protein of caveolae microdomains. Detergent-free purification of caveolae microdomains. *J. Biol. Chem.* **271**, 9690–9697 (1996).
- Morales-Ruiz, M. *et al.* Vascular endothelial growth factor-stimulated actin reorganization and migration of endothelial cells is regulated via the serine/threonine kinase Akt. *Circ. Res.* **86**, 892–896 (2000).
- Ziche, M. *et al.* Nitric oxide synthase lies downstream from vascular endothelial growth factor-induced but not basic fibroblast growth factor-induced angiogenesis. *J. Clin. Invest.* **99**, 2625–2634 (1997).
- Flanagan, J.G. & Cheng, H.J. Alkaline phosphatase fusion proteins for molecular characterization and cloning of receptors and their ligands. *Methods Enzymol.* **327**, 198–210 (2000).
- Yu, J., Rudic, R.D. & Sessa, W.C. Nitric oxide-releasing aspirin decreases vascular injury by reducing inflammation and promoting apoptosis. *Lab. Invest.* **82**, 825–832 (2002).